Supporting Information

Bioinspired Crystallization Refinement Strategy Enables Ion-Conductive Elastomers with an Ultra-Wide Strain-Insensitive Window for Reliable Signal Transmission and Adaptive Sensing

Bai Huang*, Zongming Lv, Meilin Zhang, Huidong Liu, Jiang Liu, Chaofan Liu, Hongping Li, Lihua Fu, Baofeng Lin, Chuanhui Xu

School of Chemistry and Chemical Engineering, Guangxi University, No. 100, Daxuedong Road, Xixiangtang District, Nanning 530004, China

*Corresponding author: Bai Huang, E-mail: *huangbai@gxu.edu.cn*

Table of Contents:

1. Experimental Section

1.1. Materials

Waterborne polyurethane emulsion (WPU) was purchased from Anhui Dawei Huatai New Material Technology Co., Ltd. (Hefei, China), which is translucent emulsion in an oil-in-water state, with PH value of 6-9 and solid content of 35 wt.%. Poly(diallyldimethylammonium chloride) solution (PDD, *Mw*=200000-350000, 20 wt.% in water) and tannic acid (TA, AR, 98%) were purchased from Shanghai Macklin Biochemical Technology Co., Ltd. (Shanghai, China). Cationic cellulose nanofibers (C-CNF, 1 wt.% in water) are provided by Cellunano Technology Co., Ltd. (Guilin, China). All materials were used as received.

1.2. Preparation of solid-state ionic conductive elastomer composites

A certain amount of C-CNF suspension was dispersed in 19g PDD solution by ultrasound and stirring. Then, WPU emulsion with solid mass ratio of WPU: PDD=2:1 was added and stirred for 30 minutes. Finally, 5 wt.% TA was added to obtain a homogeneous mixture. The mixed emulsion was poured into a PTFE mold to evaporate water, and further hot pressed at 130 °C for 5 min to prepare the elastomer composites. A series of samples were prepared based on the difference in the amount of C-CNF added, named PUPD-X, where X (0, 0.25, 0.50, 0.75, and 1.00) is the mass percentage of C-CNF.

1.3. Preparation of PUPD-based sensors

The PUPD-0.50 ionic conductors with dimensions of 10 × 30 mm^2 was sandwiched between two layers of insulating tape, and copper strips at both ends were used to connect the PUPD-0.50 to the output metal wire.

1.4. Characterization

1.4.1. Fourier transform infrared (FTIR) spectroscopy

Fourier transform infrared (FTIR) spectroscopic measurements were carried out using a model TENSOR II (BRUKER, Germany) with a wavenumber range of 4000-400 cm^{-1} and 32 scans were performed with a resolution of 4 cm^{-1}.

1.4.2. X-ray photoelectron spectroscopy (XPS)

X-ray photoelectron spectroscopy (XPS) characterization was recorded by K-Alpha (Thermo Scientific, USA) using Al Kα rays as the X-ray source. The C1s peak (284.8 eV) was referenced to calibrate the bond energy standard.

1.4.3. Scanning electron microscopy (SEM)

The morphology of the elastomer composites was analyzed using a field emission scanning electron microscope FEI Quattro S (Thermo Fisher, USA). The samples were sprayed with gold on the prepared samples for 90 s. The observation of the samples was carried out in high vacuum mode with an accelerating voltage of 7 kV. And elemental analysis was conducted using an energy-dispersive X-ray spectroscopy (EDS) analyzer.

1.4.4. X-ray diffraction (XRD) analysis

X-ray diffraction (XRD) analysis of the elastomer composites was characterized on an X-ray diffractometer (Rigaku D/MAX 2500 V) using Cu-Kα radiation (40 kV, 40 mA) in the 2θ range of 5° to 60°.

1.4.5. Small-angle X-ray scattering (SAXS) and wide-angle X-ray scattering (WAXS) tests

The SAXS and WAXS test was conducted on the Xeuss 3.0 SAXS/WAXS instrument using an Eiger2R 1M detector with a pixel edge length of 75 μ m. Use copper target X-rays (energy 8.05 keV, wavelength 1.54189 Å) as the light source. The testing conditions are a vacuum environment (<1 mbar) with a room temperature of approximately 24 ° C. The distance between the sample and the detector is 1000 mm, and the center coordinates of the light spot are x=540.1 and z=639.4.

1.4.6. Mechanical tests

Samples cut into dumbbell shape were tested in tensile at a rate of 50 mm/min using an electronic universal materials testing machine Instron 2360 (Instron Corporation, USA) with a 500 N transducer. The length of the dumbbell shaped specimen is 18 mm, the width is 4mm, and the thickness is measured using a vernier caliper. To ensure the correctness of the experimental results, the tensile test was performed at least three times for each specimen.

1.4.7. Ionic conductivity tests

The samples were cut into long, wide and thick slices of 10 mm×10 mm×1 mm and clamped with stainless steel sheets. Then, the ionic conductivity was tested using Jiangsu Donghua DH70000 electrochemical workstation at 25 ± 2 °C and a relative humidity of 55 ± 5%. The test method was constant potential EIS, and the frequency range was from 1 Hz to 10^6 Hz. Each specimen was carried out for at least three trials. The formula for calculating ionic conductivity is as follows:

$$\rho^{-1} = \frac{L}{R \times S} \qquad Eq.(1)$$

where ρ^{-1} is the ionic conductivity of the sample in S/m; L is the thickness of the sample in m; R is the resistance of the sample, which is equivalent to the real impedance of the sample in Ω; and S is the contact area of the sample with the stainless steel sheet in m^2.

1.4.8. Antibacterial tests

Single colonies of Escherichia coli and Staphylococcus aureus were first cultured separately on standard LB agar plates under aseptic conditions. The bacterial solution was diluted with sterile PBS solution to 10^6 CFU/mL, and then 100 μL was evenly spread onto LB solid culture medium. Sterilized samples with a diameter of 8 mm were attached to the surface of the culture medium, and then the culture dishes were placed in a constant temperature incubator at 37 ℃ for 24 hours. After cultivation, they were taken out and photographed with a regular camera, and the size of the inhibition zone was measured and recorded.

1.4.9. Gauge factor (GF) and sensing tests

The Keithley DMM 7510 multimeter was used to record the real-time resistance of PUPD-0.50 samples under tensile strain or contact/non-contact stimulation. Gauge factor (GF) was calculated as follows:

$$GF = \frac{(R - R_0)/R_0}{\varepsilon} = \frac{\Delta R/R_0}{\varepsilon}$$

where GF is the sensitivity factor, dimensionless. R_0 is the initial resistance of the sample, R is the real-time resistance of the sample in Ω.

1.4.10. Signal transmission tests

Various alternating voltage signals were generated from a signal generator (2015H, VICTOR) and transmitted through two fibers to a signal acquisition system (Donghua DH70000).

1.4.11. Density functional theory (DFT) simulation

DFT calculation is used to evaluate the electrostatic potential distribution and binding energy of three components (WPU, PDD, and C-CNF). Material studio was used to construct molecular models and performed geometry optimization in the DMol3 module. The generalized gradient approximation (GGA) function proposed by Perdew, Burke, and Ernzerhof (GGA-PBE) was used to describe the exchange-correlation potential energy[1]. The iterative tolerances for energy change, force and displacements were 1×10^{-5} Ha, 0.002 Ha/Å^{-1} and 0.005 Å, respectively. In the self-consistent field (SCF) procedure, 10^{-6} a.u. was used for the convergence standard electron density.

Fig. S1-S20

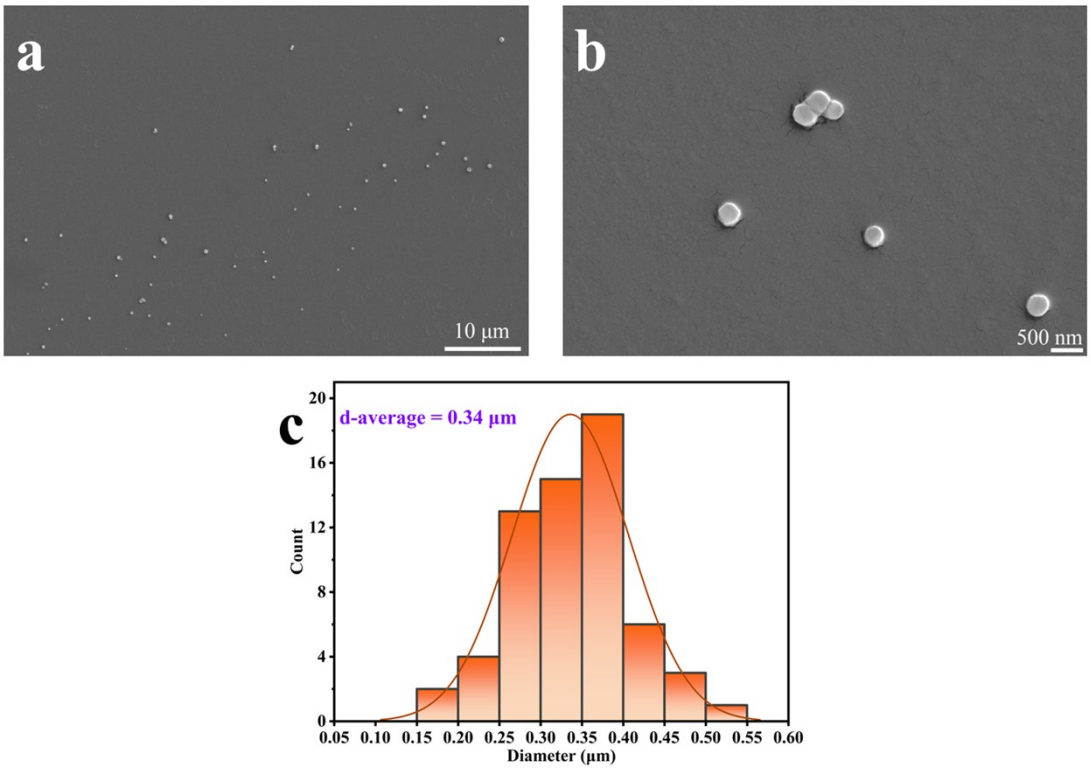

Fig. S1 SEM photos (a and b) and diameter distribution (c) of latex particles in WPU emulsion.

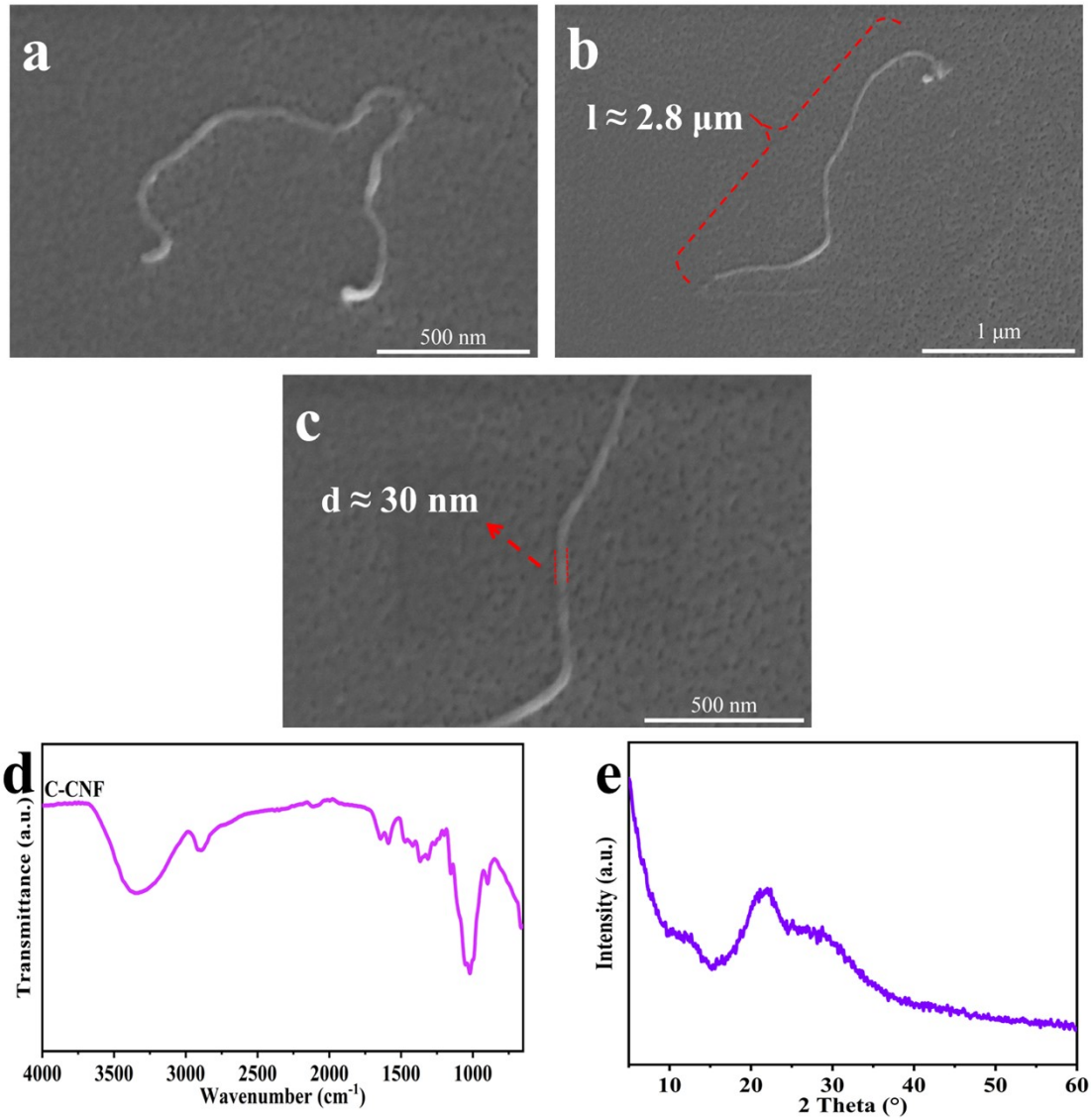

Fig. S2 SEM photos (a, b and c), FTIR spectra (d) and XRD pattern (e) of C-CNF.

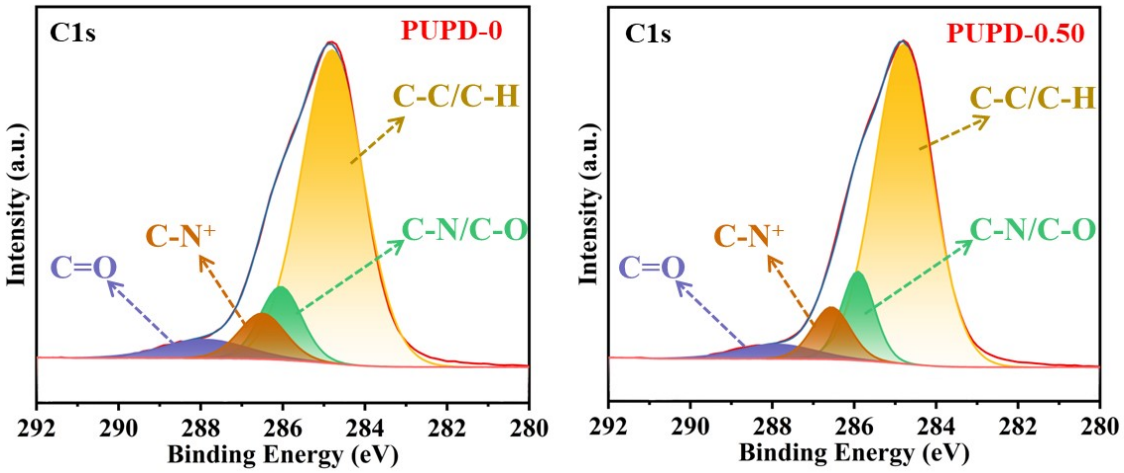

Fig. S3 XPS spectra of C 1s for PUPD-0 and PUPD-0.50 samples.

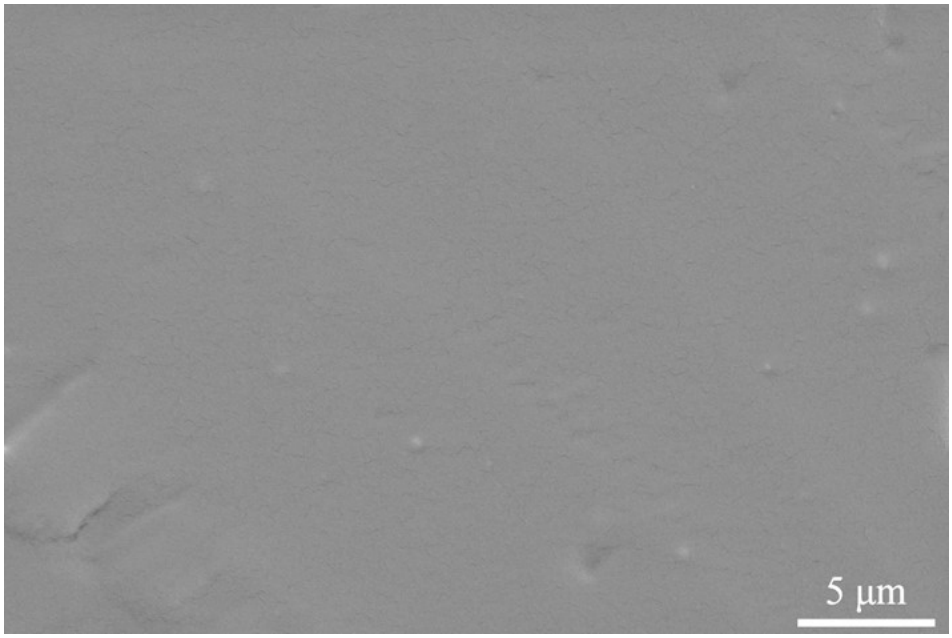

Fig. S4 SEM photo of pure WPU film.

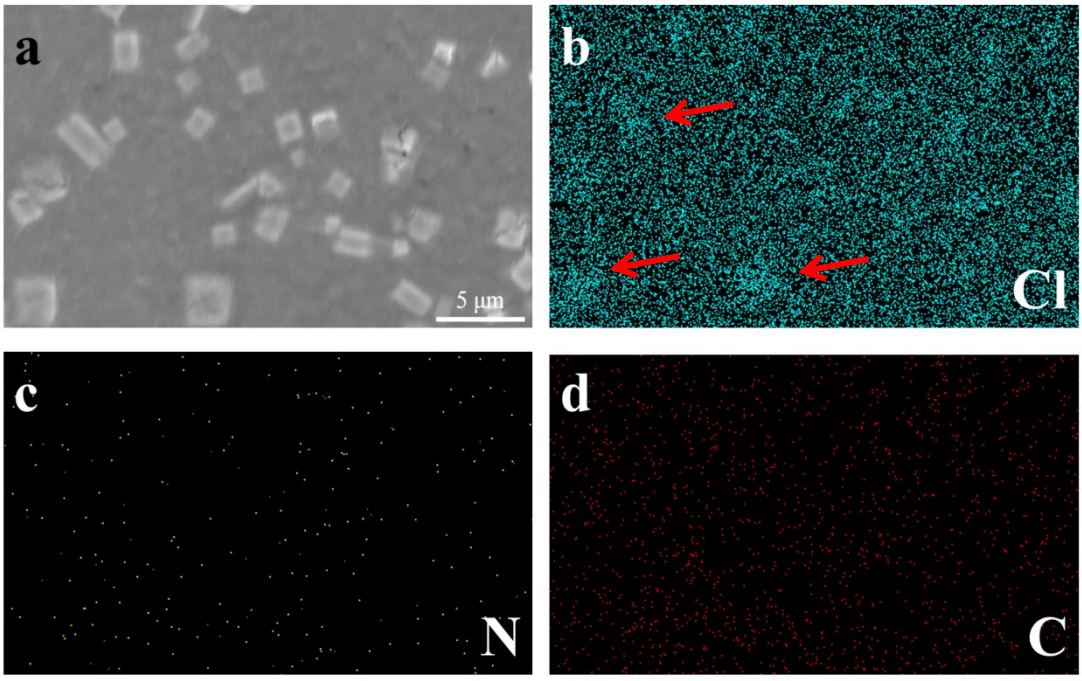

Fig. S5 SME photo (a) and element distribution (b: Cl, c: N, d: C) of pure PDD film.

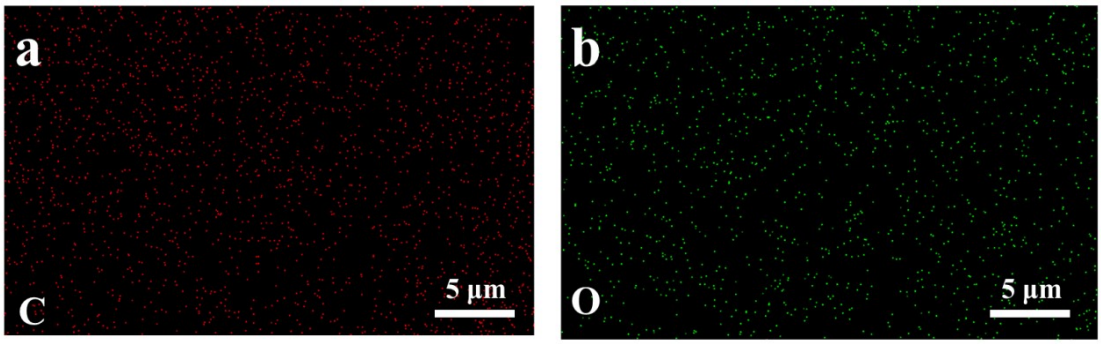

Fig. S6 C and O element distribution corresponding to SEM photo of PUPD-0.50 (Figure 2b).

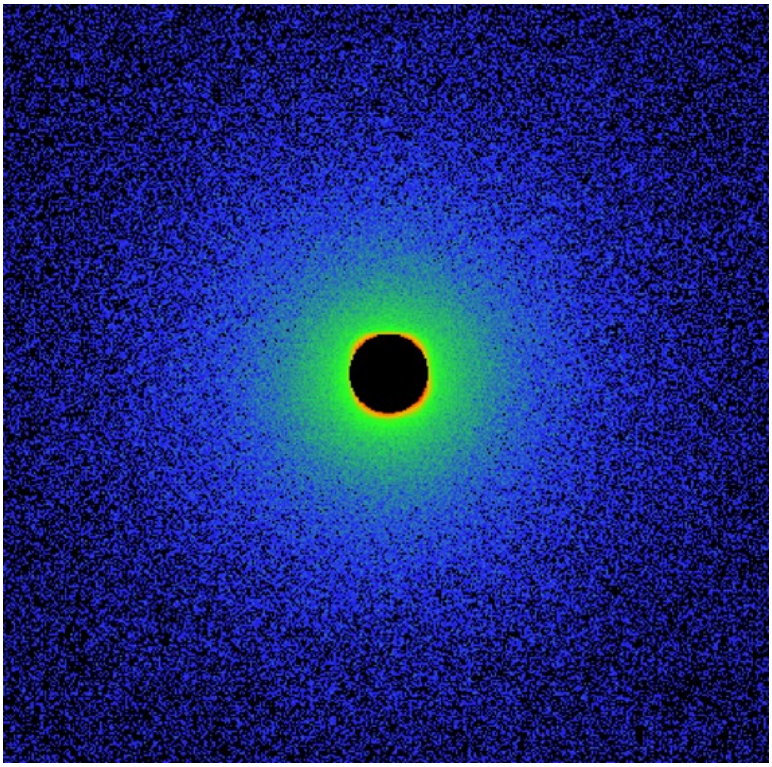

Fig. S7 2D SAXS patterns of pure WPU film.

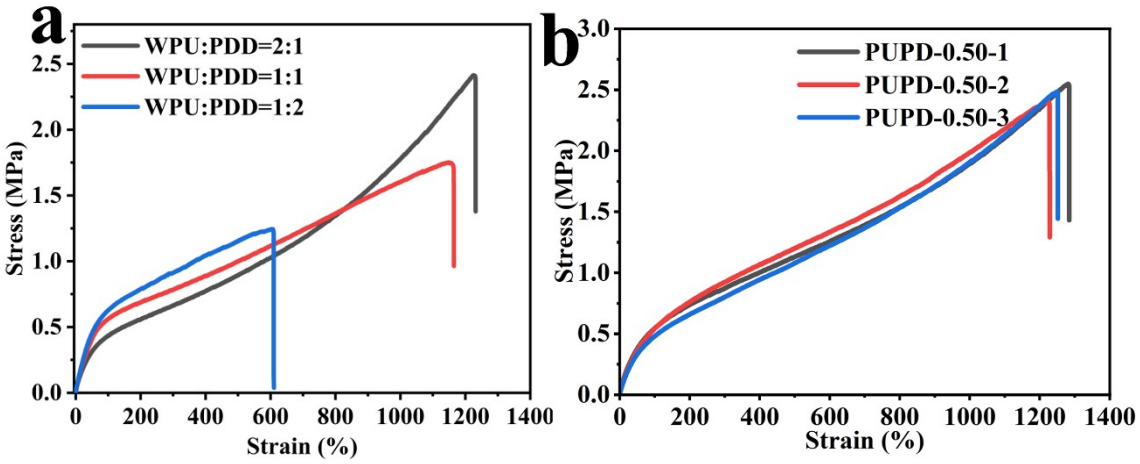

Fig. S8 Typical stress-strain curves (a) of composite films with different mass ratios of WPU and PDD, stress-strain curves (b) of three PUPD-0.50 samples.

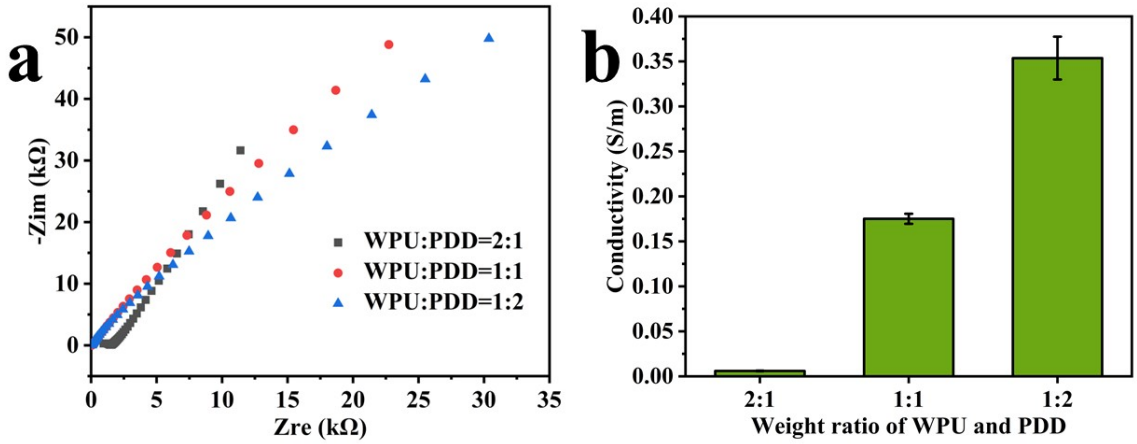

Fig. S9 Electrochemical impedance spectroscopy (EIS, a) and conductivity (b) of composite films with different mass ratios of WPU and PDD.

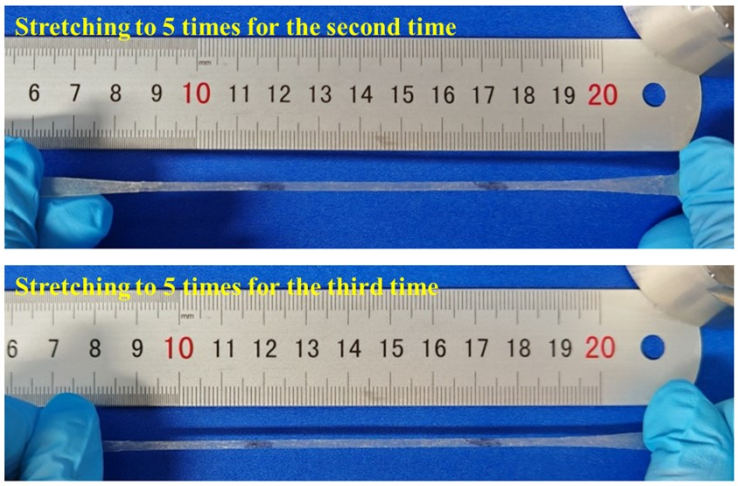

Fig. S10 Photos of PUPD-0.50 stretched for the second and third time.

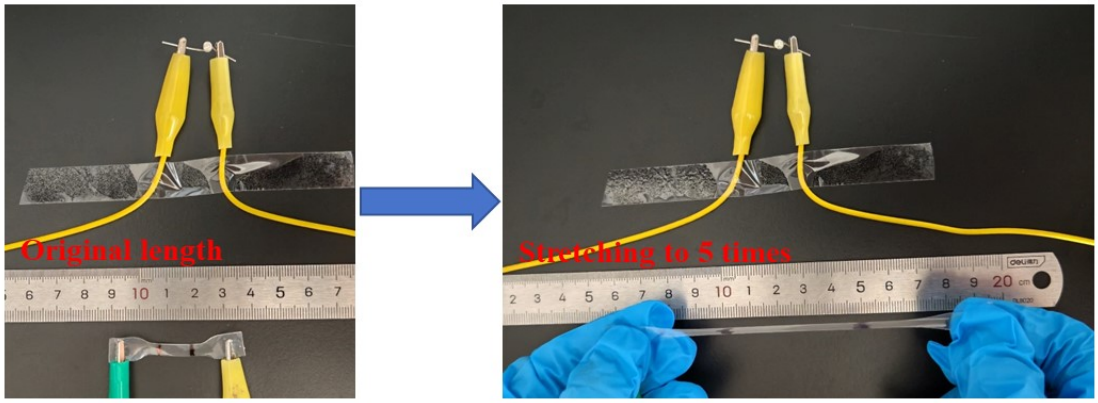

Fig. S11 Pure WPU film cannot light up LED light at its original length or when stretched to 5 times.

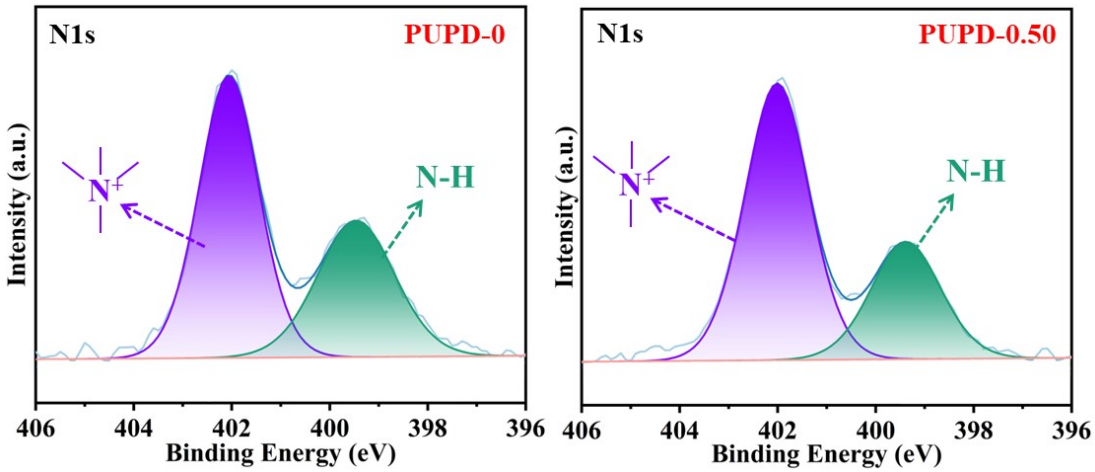

Fig. S12 XPS spectra of N 1s for PUPD-0 and PUPD-0.50 samples.

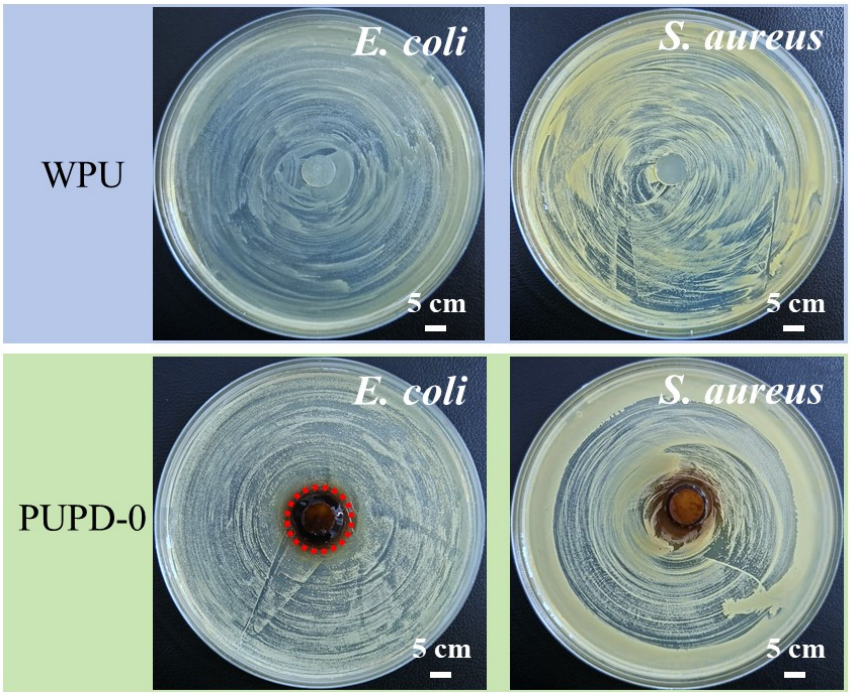

Fig. S13 Antibacterial activity of pure WPU and PUPD-0 against *Escherichia coli* and *Staphylococcus aureus*.

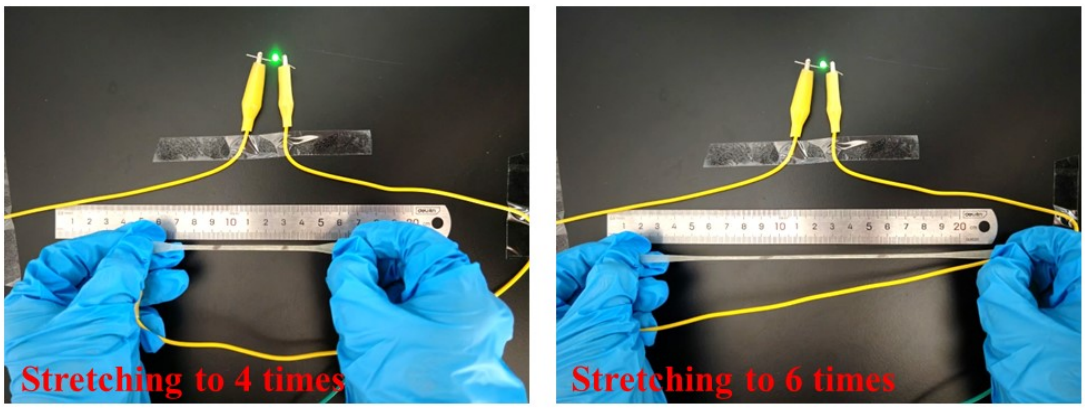

Fig. S14 Photos of PUPD-0.50 lighting up LED lights at different stretching ratios.

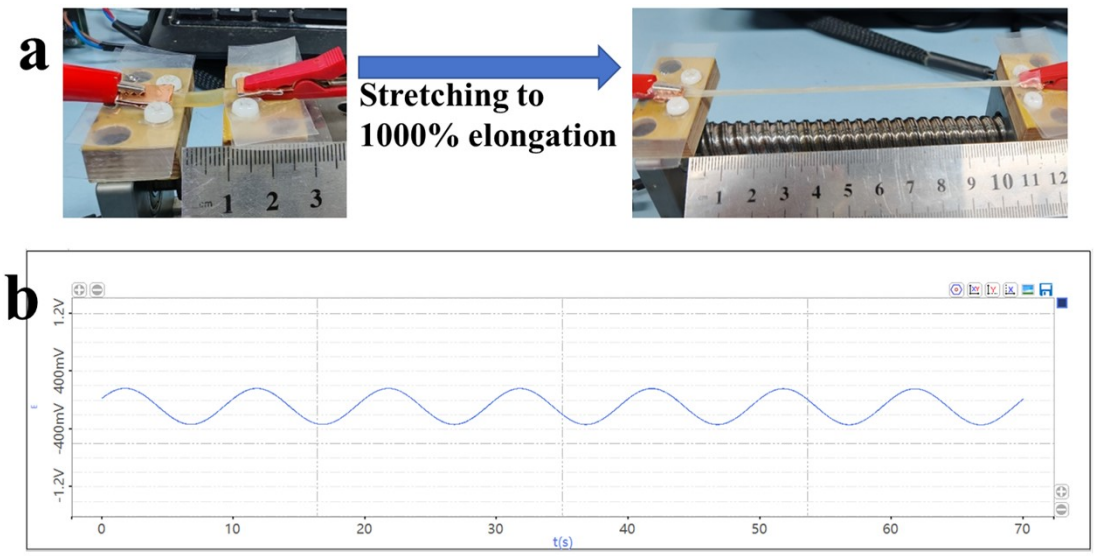

Fig. S15 PUPD-0.50 performs AC voltage signal transmission at 1000% strain (a) and corresponding signals (b).

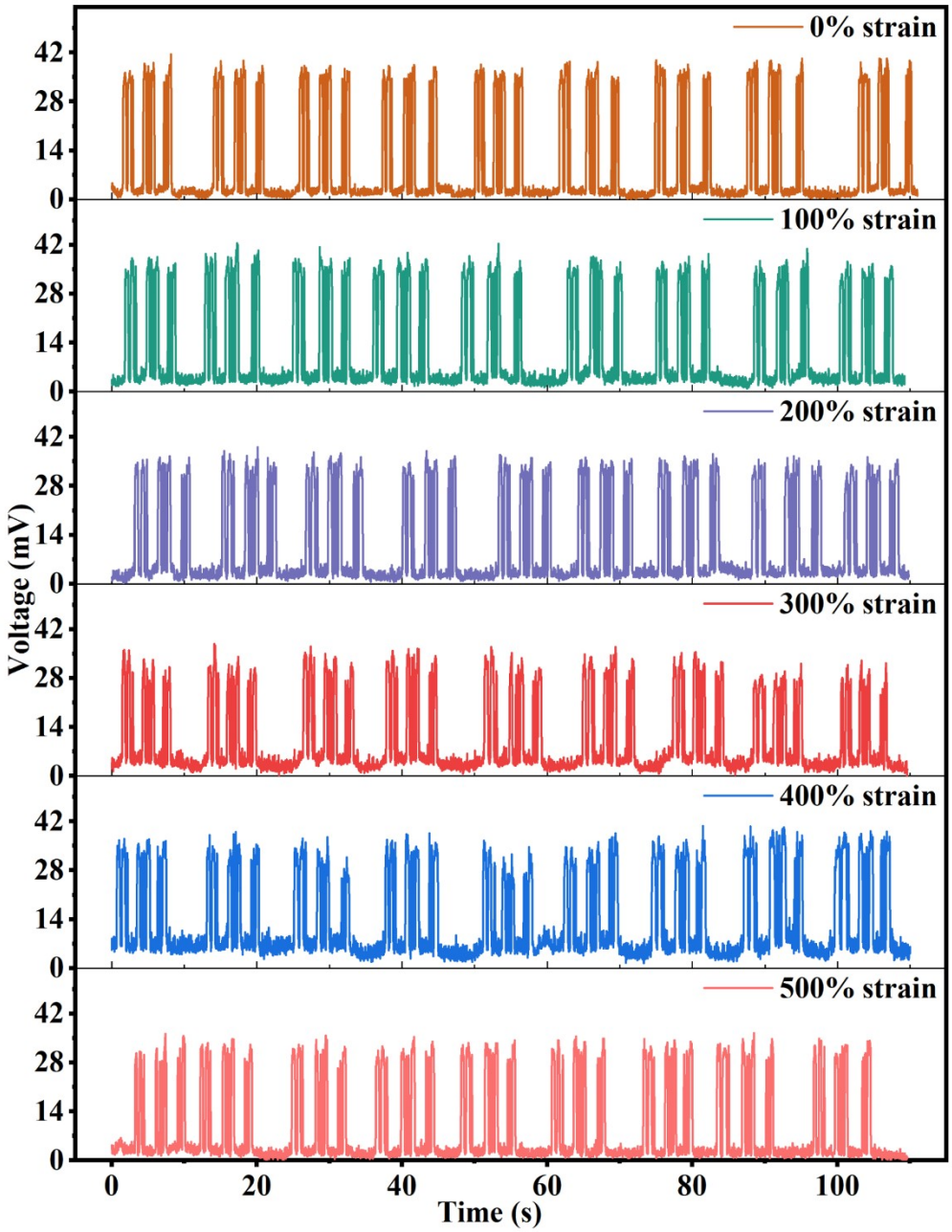

Fig. S16 The "GXU" Morse code was cyclically sent by clicking on the sensor at different strain levels.

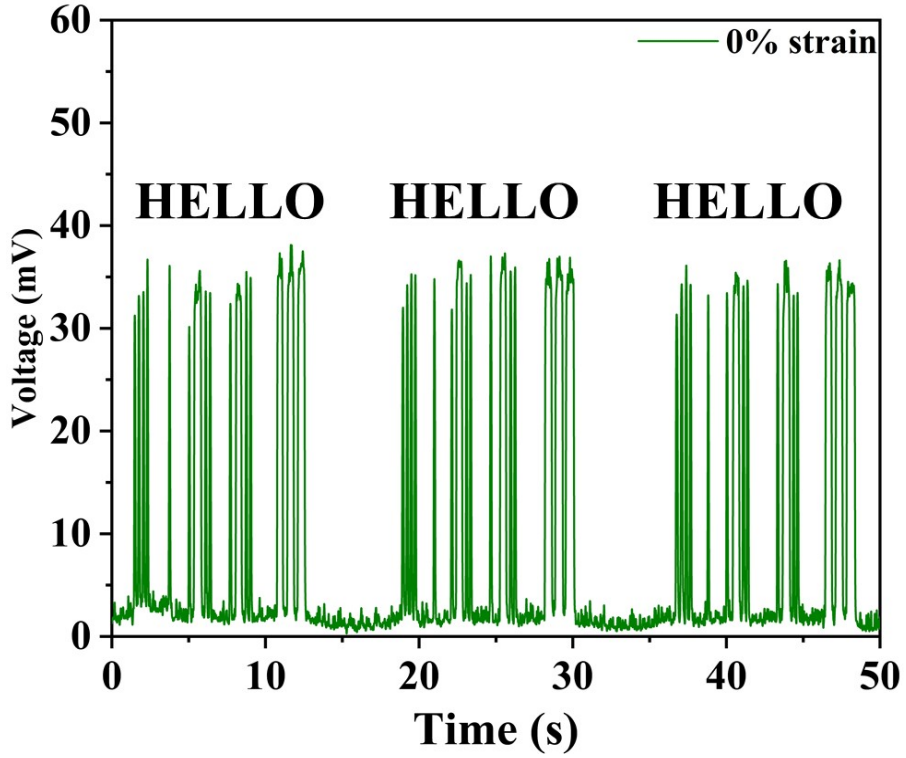

Fig. S17 Under 0% strain level, the "HELLO" Morse code was cyclically sent by clicking on the sensor.

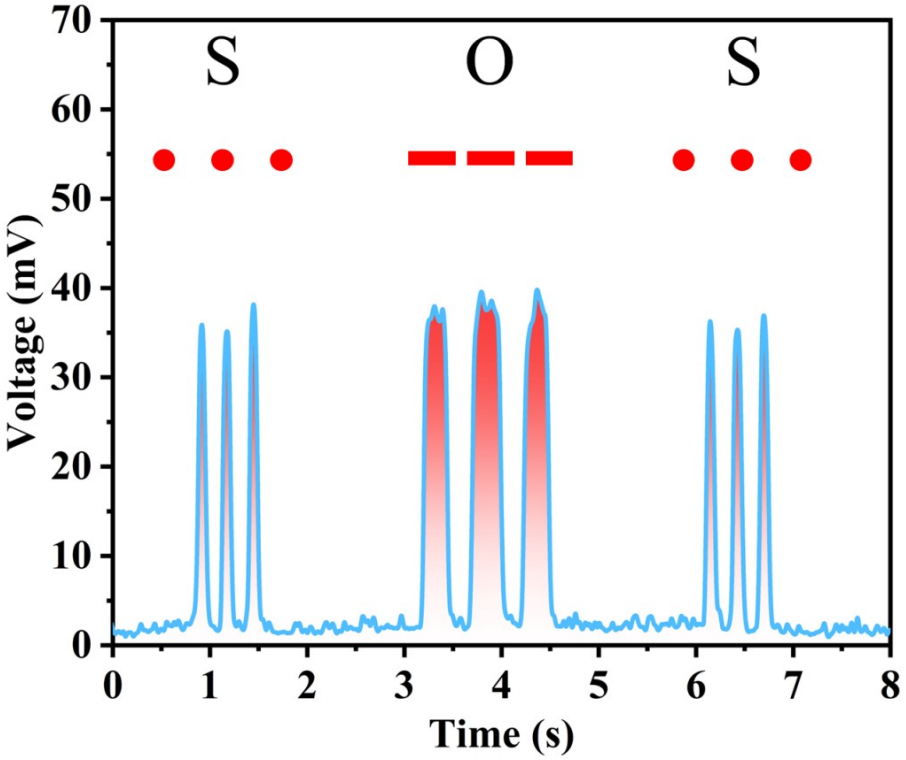

Fig. S18 Morse code “SOS” sent by clicking on the sensor under 0% strain.

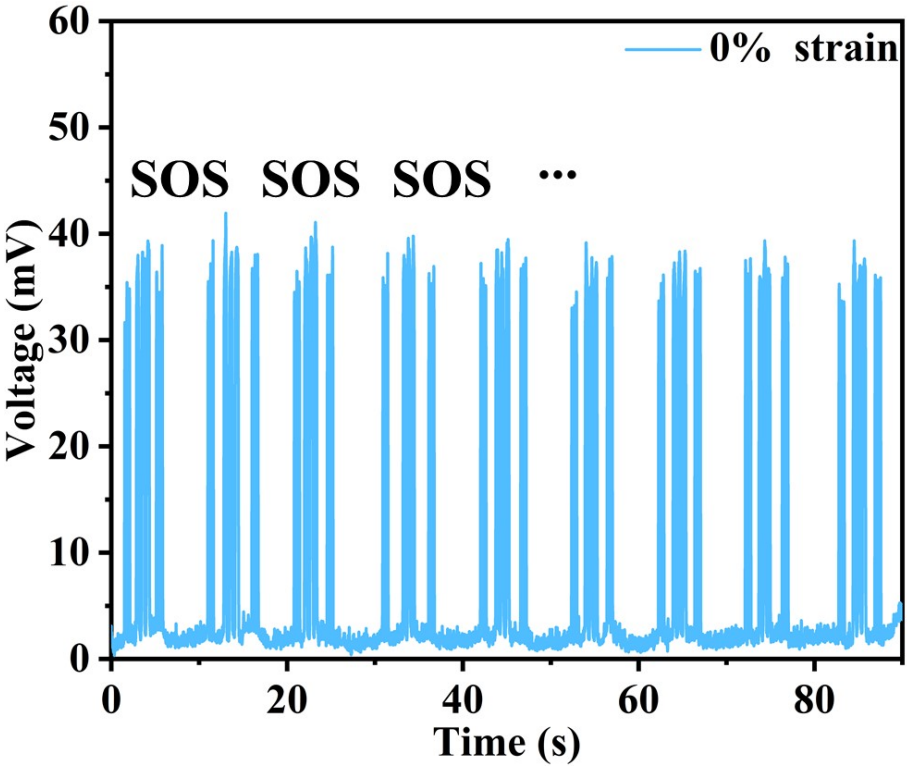

Fig. S19 Under 0% strain level, the "SOS" Morse code was cyclically sent by clicking on the sensor.

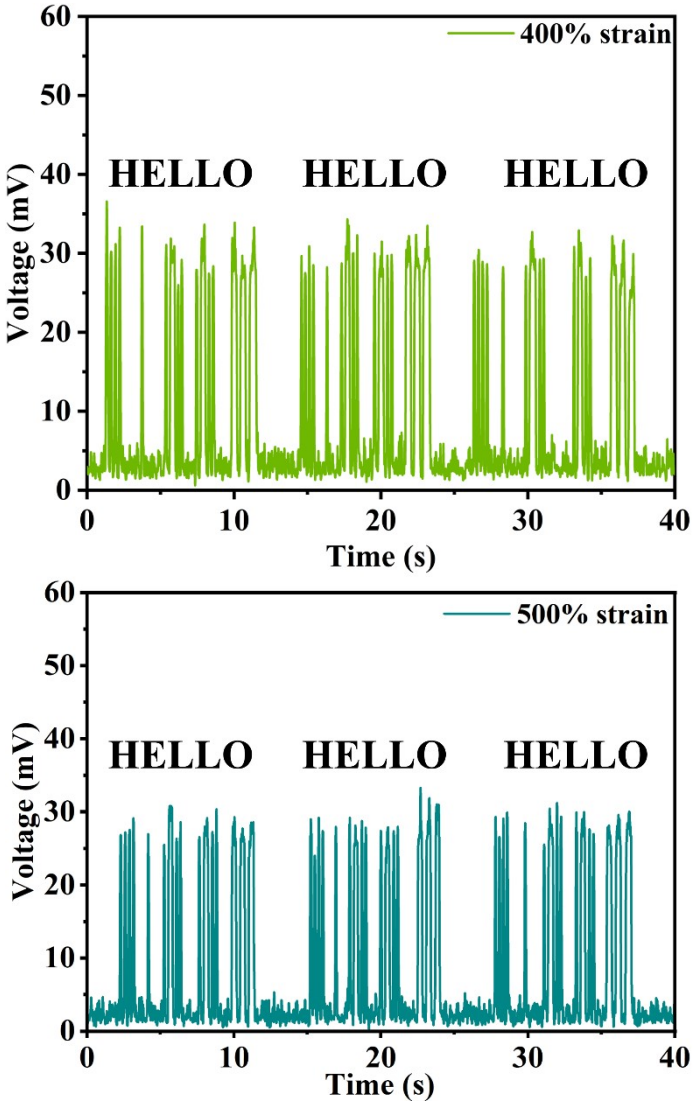

Fig. S20 Under 400% and 500% strain level, the "HELLO" Morse code was cyclically sent by clicking on the sensor.

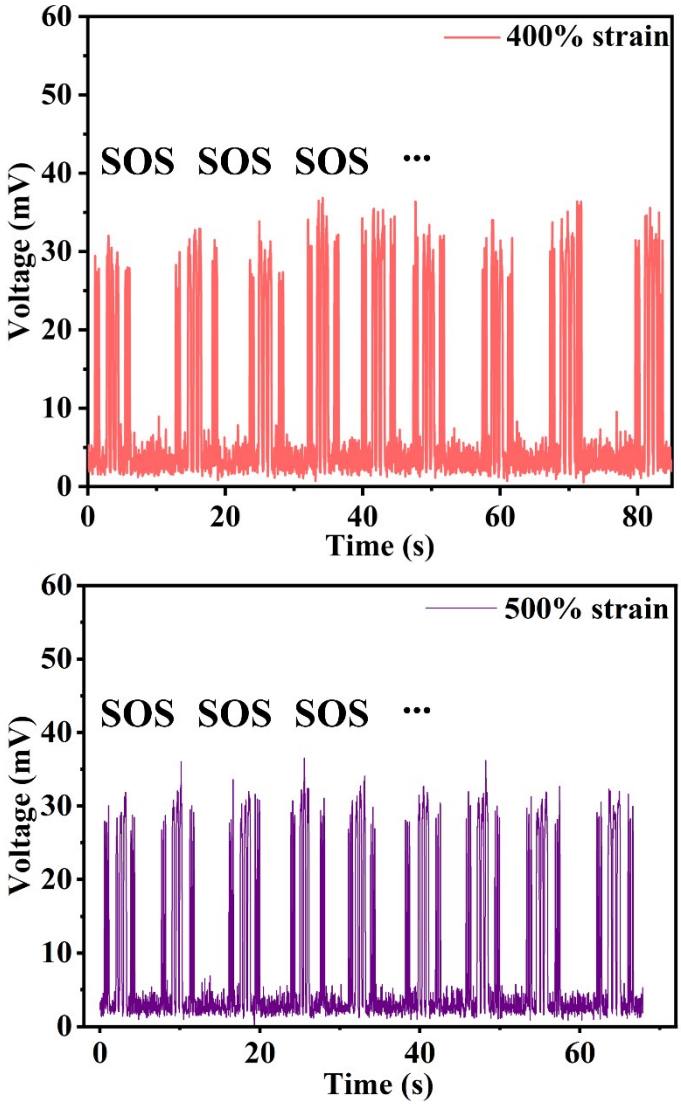

Fig. S21 Under 400% and 500%strain level, the "SOS" Morse code was cyclically sent by clicking on the sensor.

Table S1

Table S1. Comparison of performance between PUPD-0.50 and reported strain-insensitive conductors

Samples	Sress (MPa)	Toughness (MJ/m^3) [a]	Strain insensitive window (%)	Gauge factor (GF) [b]
Ref.3[2]	0.4	1.1	500	0.04 (0-200%)
Ref.4[3]	11.58	10.8	100	-
Ref.11[4]	0.25	0.219	70	-
Ref.12[5]	0.5	1.25	200	0.04 (0-200%)
Ref.14[6]	10.16	82.06	600	0.05 (0-600%)
Ref.15[7]	12.6	26.64	143	0.11 (0-143%)
Ref.16[8]	3.9	8.2	30	-
Ref.17[9]	7.63	36.21	50	0.02 (0-50%)
Ref.18[10]	2.17	10.29	250	0.29 (0-200%)
Ref.19[11]	21.8	5.79	53	0.20 (0-30%)
Ref.20[12]	1.2	0.73	50	-
Ref.21[13]	23	0.11	20	1.33 (0-15%)
Ref.25[14]	0.329	0.00493	60	-
Ref.27[15]	8.0	29.3	30	3.35 (0-700%)
Ref.28[16]	-	-	50	0.02 (0-140%)
Ref.29[17]	0.047	0.07	75	1.04 (0-75%)
This work	2.48	17.16	1200	0.06 (0-450%) 0.10 (450%-1000%) 0.12 (1000%-1200%)

[a] In the absence of parameter values in the paper, approximate values were estimated through stress-strain curves.

b In the absence of parameter values in the paper, approximate values are estimated using resistance and strain data.

Movie S1-S3

Movie S1

PUPD-0.50 performs sinusoidal AC signal transmission when stretched to 1000% strain.

Movie S2

Sensors based on PUPD-0.50 conductors can generate clear and stable voltage signals in both contact and non-contact modes.

Movie S3

Sensors based on PUPD-0.50 conductors was used for non-contact switching to control the lighting and extinguishing of LED.

References

(1) Xu, Q.; Hou, M.; Wang, L.; Zhang, X.; Liu, L. Anti-bacterial, anti-freezing starch/ionic liquid/PVA ion-conductive hydrogel with high performance for multi-stimulation sensitive responsive sensors. *Chemical Engineering Journal* **2023,** *477,* 147065.

(2) Ye, H.; Wu, B.; Sun, S.; Wu, P. A solid-liquid bicontinuous fiber with strain-insensitive ionic conduction. *Adv. Mater.* **2024,** *36,* 2402501.

(3) Zhao, Y.; Wang, B.; Tan, J.; Yin, H.; Huang, R.; Zhu, J.; Lin, S.; Zhou, Y.; Jelinek, D.; Sun, Z.; Youssef, K.; Voisin, L.; Horrillo, A.; Zhang, K.; Wu, B. M.; Coller, H. A.; Lu, D. C.; Pei, Q.; Emaminejad, S. Soft strain-insensitive bioelectronics featuring brittle materials. *Science* **2022,** *378,* 1222–1227.

(4) Zhang, L.; Gao, Z.; Lei, H.; Liu, Y.; Yi, J.; Wang, A.; Gu, H.; Shi, J.; Zhang, P.; Wen, Z.; Sun, X. Strain-insensitive stretchable triboelectric tactile sensors via interfacial stress dispersion. *Nano Energy* **2025,** *133,* 110482.

(5) Ma, J.; Liu, Z.; Zhang, P. Precisely patterning liquid metal microfibers through electrohydrodynamic printing for soft conductive composites and electronics. *Adv. Mater.* **2025,** *37,* 2507646.

(6) Luo, M.; Wei, W.; Guo, Q.; Zhong, W.; Jia, K.; Chang, K.; Lu, Y.; Li, M.; Wang, D. A liquid metal-embedded sheath-core fiber with internal helical structure for strain-insensitive electronics. *Adv. Sci.* **2025,** *12,* e09547.

(7) Zheng, Z.; Yu, Z.; Kong, L.; Lin, B.; Fu, L.; Xu, C. Strain/deformation-insensitive wearable rubber composite for temperature monitoring based on the photothermal and thermoelectric conversion. *Chem. Eng. J.* **2024,** *484,* 149329.

(8) Choi, S. B.; Noh, T.; Jung, S. B.; Kim, J. W. Stretchable piezoresistive pressure sensor array with sophisticated sensitivity, strain-insensitivity, and reproducibility. *Adv. Sci.* **2024,** *11,* 2405374.

(9) Jung, D.; Lim, C.; Park, C.; Kim, Y.; Kim, M.; Lee, S.; Lee, H.; Kim, J. H.; Hyeon, T.; Kim, D. H. Adaptive self-organization of nanomaterials enables strain-insensitive resistance of stretchable metallic nanocomposites. *Adv. Mater.* **2022,** *34,* 2200980.

(10) Zhang, P.; Athavale, O. N.; Zhu, B.; Travas-Sejdic, J.; Du, P. Wet-printed stretchable and strain-insensitive conducting polymer electrodes: Facilitating in vivo gastric slow wave mapping. *Adv. Mater. Technol.* **2024,** *9,* 2400849.

(11) He, H.; Chen, R.; Yue, S.; Yu, S.; Wei, J.; Ouyang, J. Salt-induced ductilization and strain-insensitive resistance of an intrinsically conducting polymer. *Sci. Adv.* **2022,** *8,* eabq8160.

(12) Park, D.; Kwak, H.; Kim, S.; Choi, H.; Lim, I.; Kwak, M.; Kim, I. S.; Park, H.; Eom, I. Y.; Lee, J. W.; Park, I.; Lee, A.; Jeong, U. Stretchable anisotropic conductive film with position-registered conductive microparticles used for strain-insensitive ionic interfacing in stretchable ionic sensors. *Adv. Funct. Mater.* **2024,** *34,* 2408902.

(13) Sharma, S.; Pradhan, G. B.; Jeong, S.; Zhang, S.; Song, H.; Park, J. Y. Stretchable and all-directional strain-insensitive electronic glove for robotic skins and human–machine interfacing. *ACS Nano* **2023,** *17,* 8355-8366.

(14) Shen, Y.; Li, Z.; Xiang, Y.; Feng, J.; Zhang, X.; Wang, T. Decoupling stretching and sensing regions to achieve strain-insensitive iontronic pressure sensors for gesture recognition. *Chem. Eng. J.* **2025,** *516,* 163763.

(15) Wang, F.; Chen, J.; Cui, X.; Liu, X.; Chang, X.; Zhu, Y. Wearable ionogel-based fibers for strain sensors with ultrawide linear response and temperature sensors insensitive to strain. *ACS Appl. Mater. Interfaces* **2022,** *14,* 30268-30278.

(16) Park, J.; Ko, Y.; Cho, J. Y.; Lee, S.; Lee, Y.; Han, J.; Ko, H. Stretchable ionic composites for strain-insensitive dual-mode pressure and proximity sensors. *Chem. Eng. J.* **2024,** *480,* 148172.

(17) Xie, F.; Lu, F.; Tian, Y.; Zhang, X.; Wang, Y.; Zheng, L.; Gao, X. Thermochromic-based bimodal sensor for strain-insensitive temperature sensing and synchronous strain sensing. *Chem. Eng. J.* **2023,** *471,* 144504.